

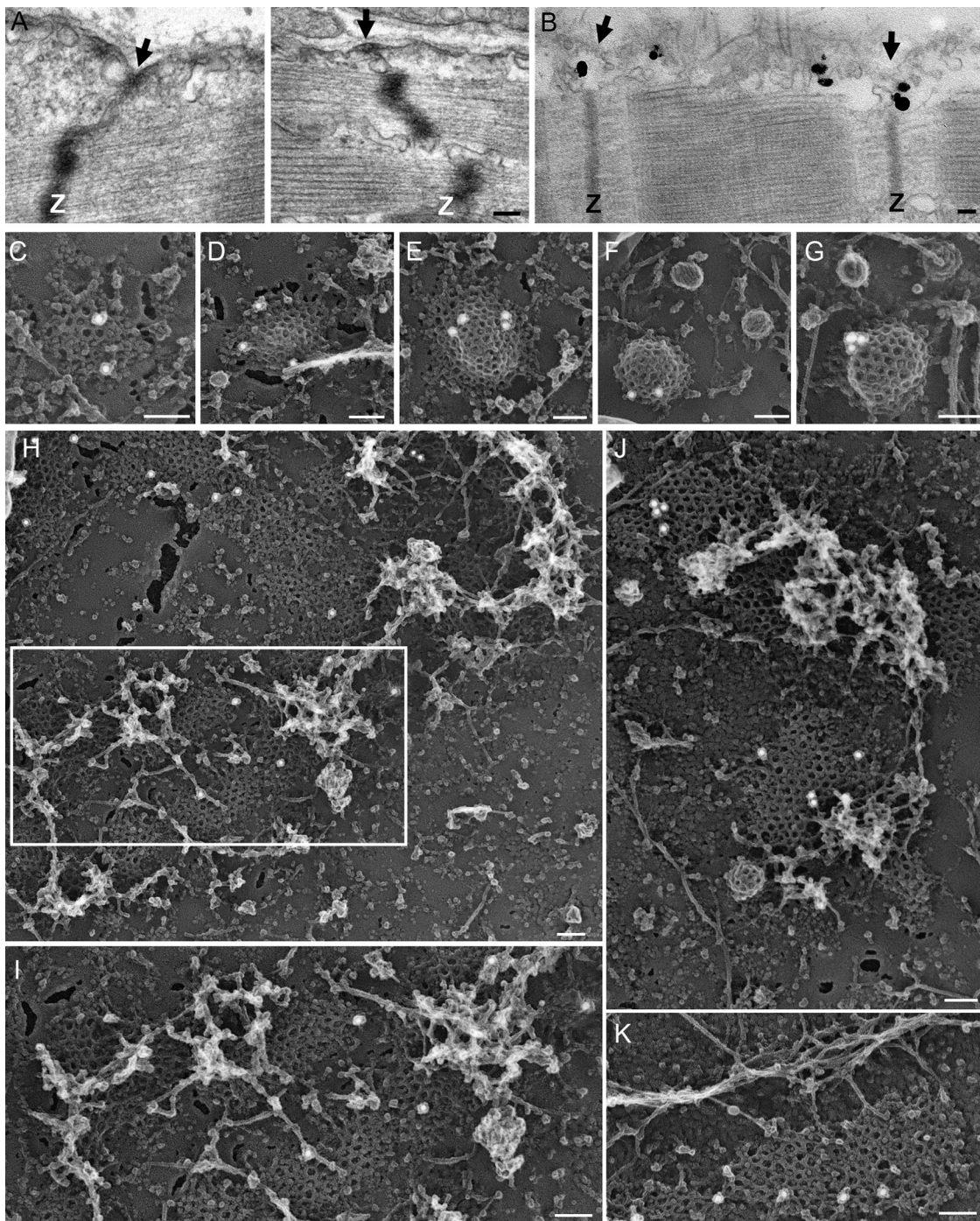
Vassilopoulos et al., <http://www.jcb.org/cgi/content/full/jcb.201309096/DC1>

Figure S1. **Ultrastructural localization of clathrin in adult skeletal muscle and mouse primary myotubes.** (A) Thin (70 nm) longitudinal muscle sections were stained with 1% tannic acid followed by uranyl acetate and lead citrate. An arrow points at electron-dense regions corresponding to costameres. Z-line position is indicated by letter Z. (B) Thin longitudinal muscle sections immunolabeled with CHC polyclonal antibody and processed for EM. (C-K) Fixed PM sheets prepared from control primary myotubes were labeled with CHC antibodies, and then with secondary antibodies conjugated to 18-nm colloidal gold particles. Representative freeze-etch images show the distribution of clathrin on small, flat, or invaginated coated pits (C-G) or on large, flat, actin-associated coated plaques (H-K). Bars, 100 nm.

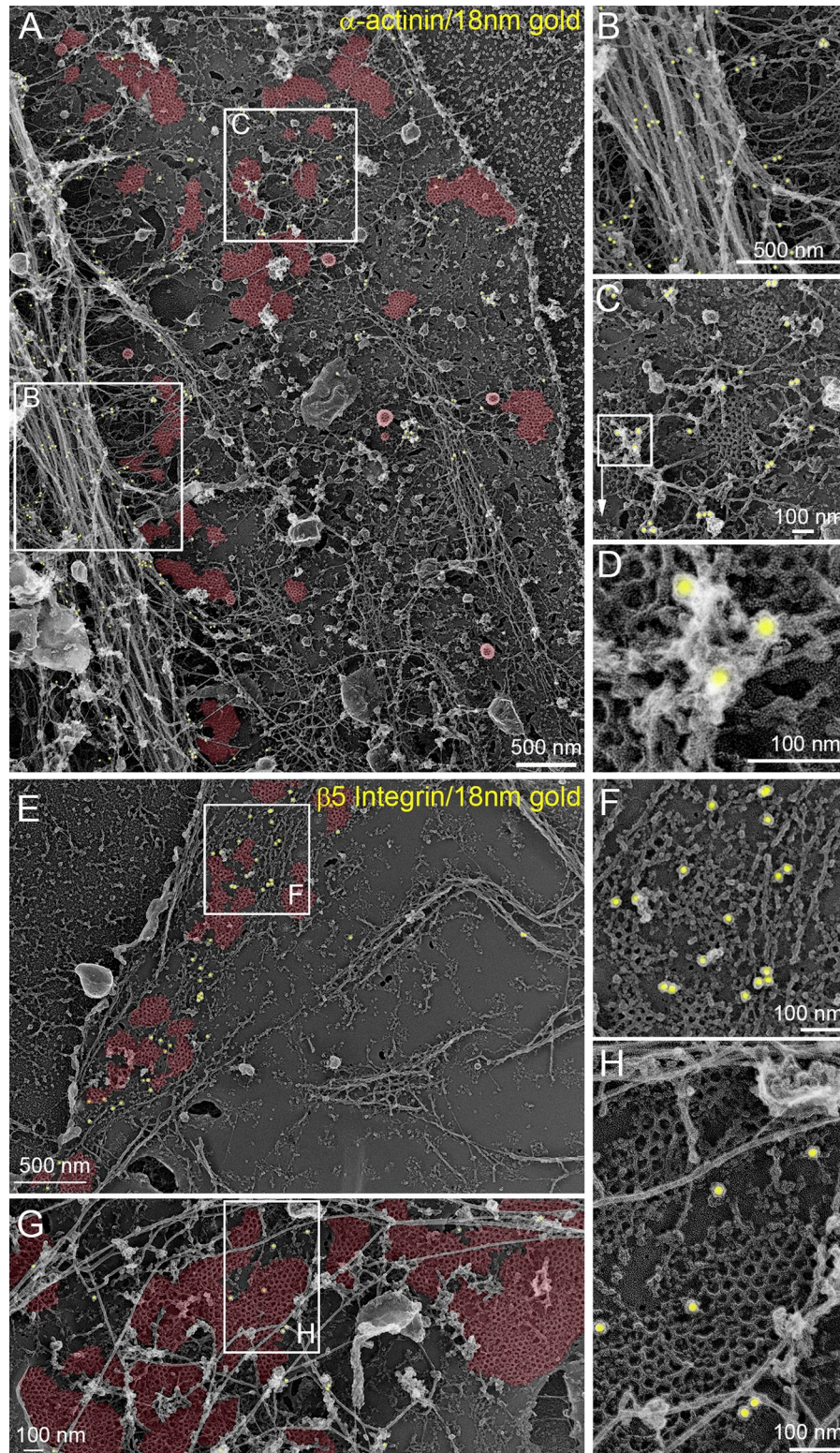


Figure S2. **Additional images of  $\alpha$ -actinin localization and localization of  $\beta$ 5-integrin in clathrin plaques.** (A–D) Adherent plasmalemmal sheets prepared from control primary mouse myotubes were labeled with  $\alpha$ -actinin antibodies followed by secondary antibodies conjugated to 18-nm colloidal gold particles (pseudocolored yellow). Note that  $\alpha$ -actinin is found on both the contractile apparatus (A and B) and on large and flat clathrin-coated lattices (A, C, and D). (E–H) Fixed PM sheets prepared from control myotubes were labeled with  $\beta$ 5-integrin antibodies, and then with secondary antibodies conjugated to 18-nm colloidal gold particles. Representative freeze-etch images show the spatial distribution of endogenous  $\beta$ 5-integrin enriched on large clathrin-coated structures. In A, E, and G, clathrin lattices are pseudocolored pale red.

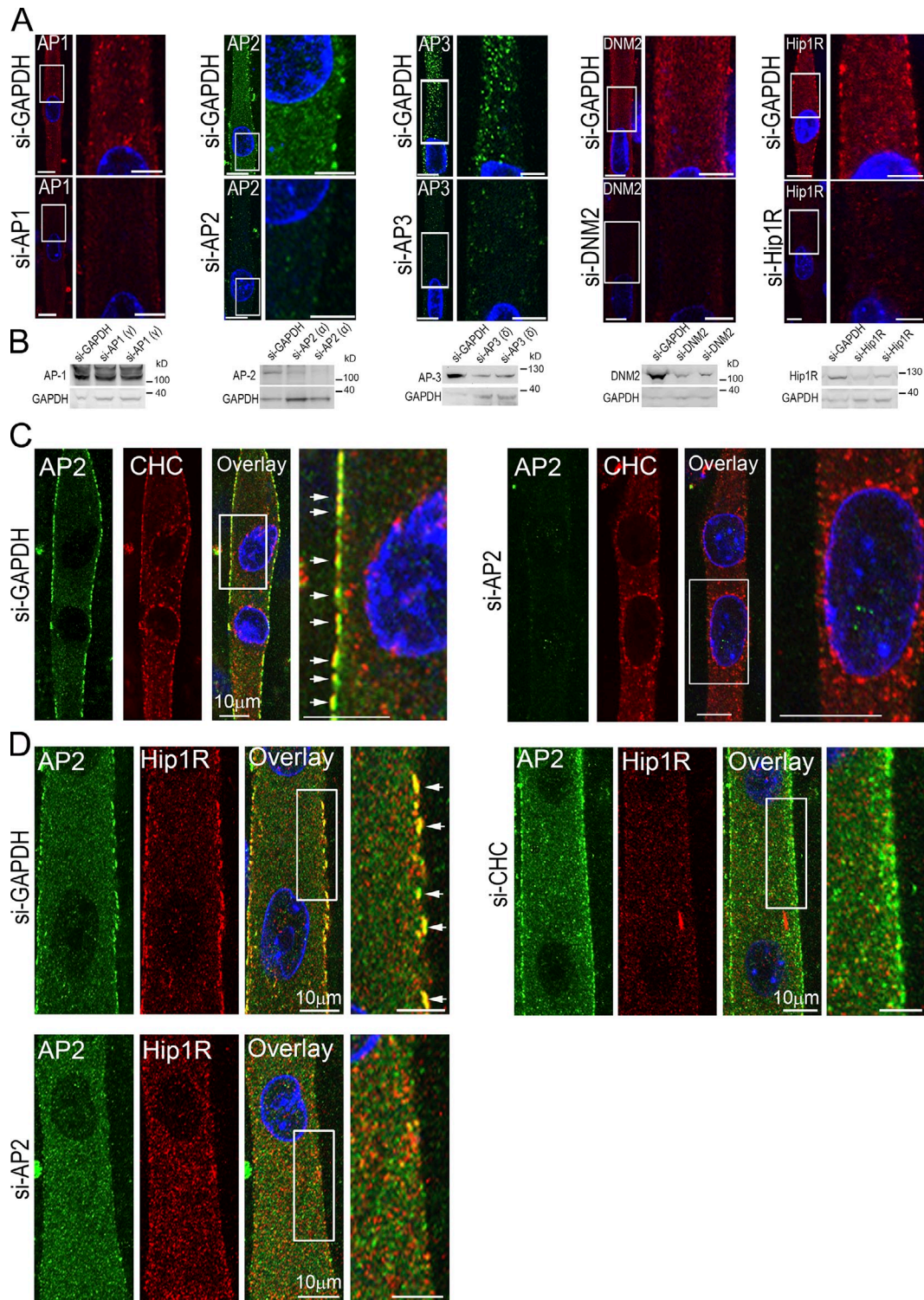


Figure S3. **siRNA-mediated depletion of AP1, AP2, AP3, DNM2, and Hip1R.** (A) Differentiated C2C12 myotubes were treated with either siRNA targeting GAPDH, the  $\gamma$ -subunit of AP1, the  $\alpha$ -subunit of AP2, the  $\delta$ -subunit of AP3, DNM2, or Hip1R. Immunofluorescent staining [DNA staining with DAPI is shown in blue (bar, 10  $\mu$ m) and the boxed region in the merged images is magnified in the insets (bar, 5  $\mu$ m)]. (B) Differentiated C2C12 myotubes were treated with either siRNA targeting GAPDH, the  $\gamma$ -subunit of AP1, the  $\alpha$ -subunit of AP2, the  $\delta$ -subunit of AP3, DNM2, or Hip1R and subjected to Western blot detection of the  $\gamma$ -subunit of AP1, the  $\alpha$ -subunit of AP2, the  $\delta$ -subunit of AP3, DNM2, or Hip1R. (C) Differentiated C2C12 skeletal muscle cells were treated with control GAPDH siRNA or siRNA against AP2 and processed for immunofluorescent staining with antibodies against the  $\alpha$ -subunit of AP2 (green) and CHC (red). DNA staining (DAPI, blue) identifies differentiated, multinucleated myotubes (bar, 10  $\mu$ m). The boxed region in the merged images is magnified in the insets (bar, 10  $\mu$ m). (D) Differentiated C2C12 myotubes were treated with either siRNA targeting GAPDH, CHC, or the  $\alpha$ -subunit of AP2 and processed for immunofluorescent staining with antibodies against the  $\alpha$ -subunit of AP2 (green) and Hip1R (red). DNA staining (DAPI, blue) identifies differentiated, multinucleated myotubes (bar, 10  $\mu$ m). The boxed region in the merged images is magnified in the insets, and arrows in C and D indicate colocalization between AP2 and CHC or AP2 and Hip1R, respectively (bar, 5  $\mu$ m).

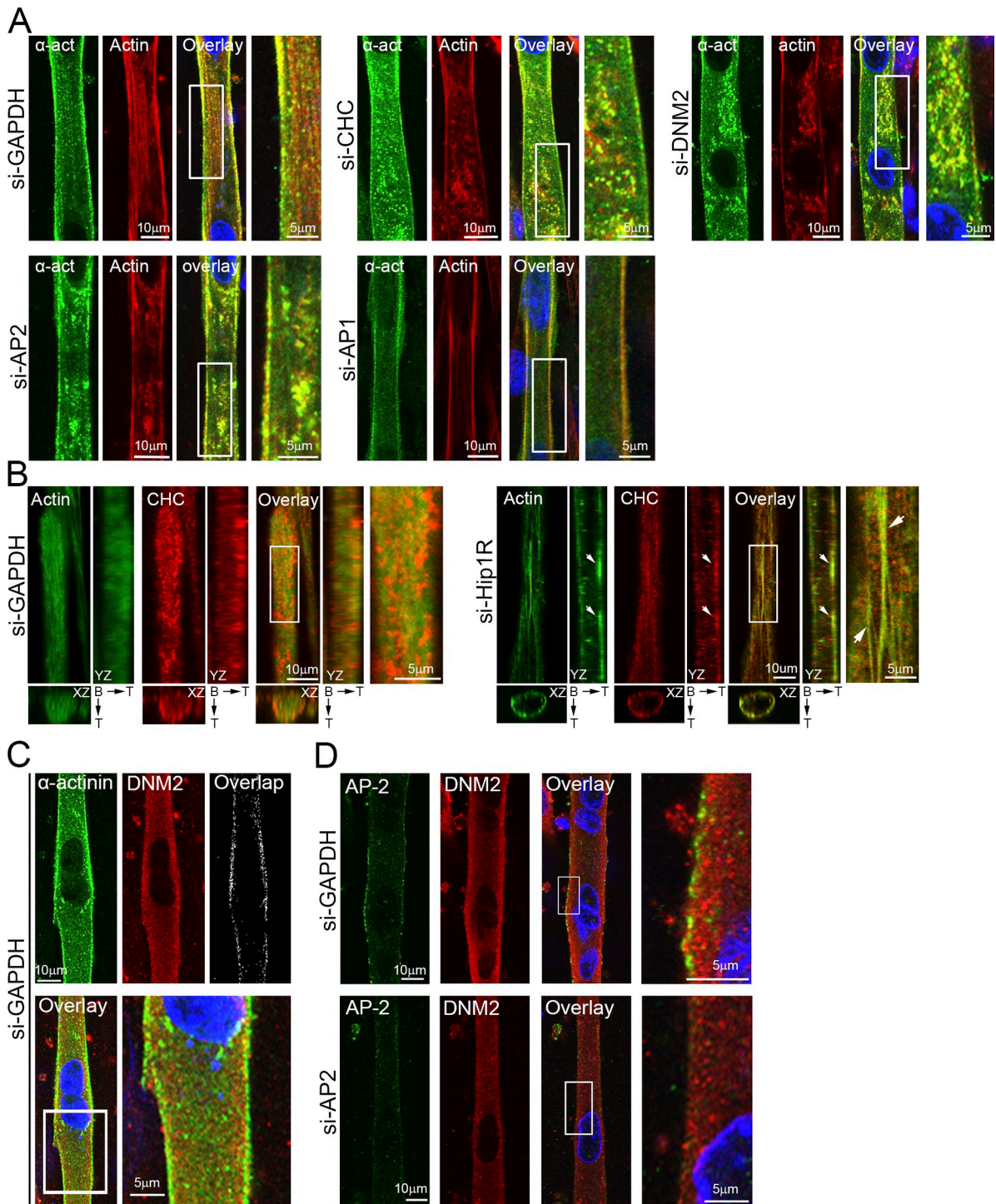


Figure S4. **Effect of siRNA-mediated depletion of CHC, AP1, AP2, Hip1R, and DNM2 on actin distribution and localization of DNM2 in control and AP2-depleted C2C12 myotubes.** (A) Differentiated C2C12 myotubes were treated with either siRNA targeting GAPDH, CHC, the  $\gamma$ -subunit of AP1, the  $\alpha$ -subunit of AP2, or DNM2 and processed for immunofluorescent staining with antibodies against  $\alpha$ -actinin (green) and treated with TRITC-phalloidin in order to label actin filaments (red). DNA staining (DAPI, blue) identifies differentiated, multinucleated myotubes. The boxed region in the merged image is magnified in the inset. (B) Differentiated C2C12 myotubes were treated with either siRNA targeting GAPDH or Hip1R and processed for immunofluorescent staining with FITC-phalloidin (green) in order to label actin filaments and antibodies against CHC (red). Bar, 10  $\mu$ m. XZ and YZ projections of serial confocal sections are shown for each individual channel and the overlay image (B, bottom; T, top). The boxed region in the overlay is magnified in the insets (bar, 5  $\mu$ m). Arrows indicate colocalization between actin filaments and CHC. (C) Immunofluorescent staining of  $\alpha$ -actinin (green) and DNM2 (red) in differentiated C2C12 myotubes treated with siRNA targeting GAPDH. DNA staining (DAPI, blue) identifies differentiated, multinucleated myotubes. The boxed region in the merged image is magnified in the inset. A black and white composite image depicting colocalized pixels between the  $\alpha$ -actinin and DNM2 staining is shown. (D) Differentiated C2C12 myotubes were treated with either siRNA targeting GAPDH or the  $\alpha$ -subunit of AP2 and processed for immunofluorescent staining with antibodies against the  $\alpha$ -subunit of AP2 (green) and DNM2 (red). DNA staining (DAPI, blue) identifies differentiated, multinucleated myotubes. The boxed region in the merged images is magnified in the insets.

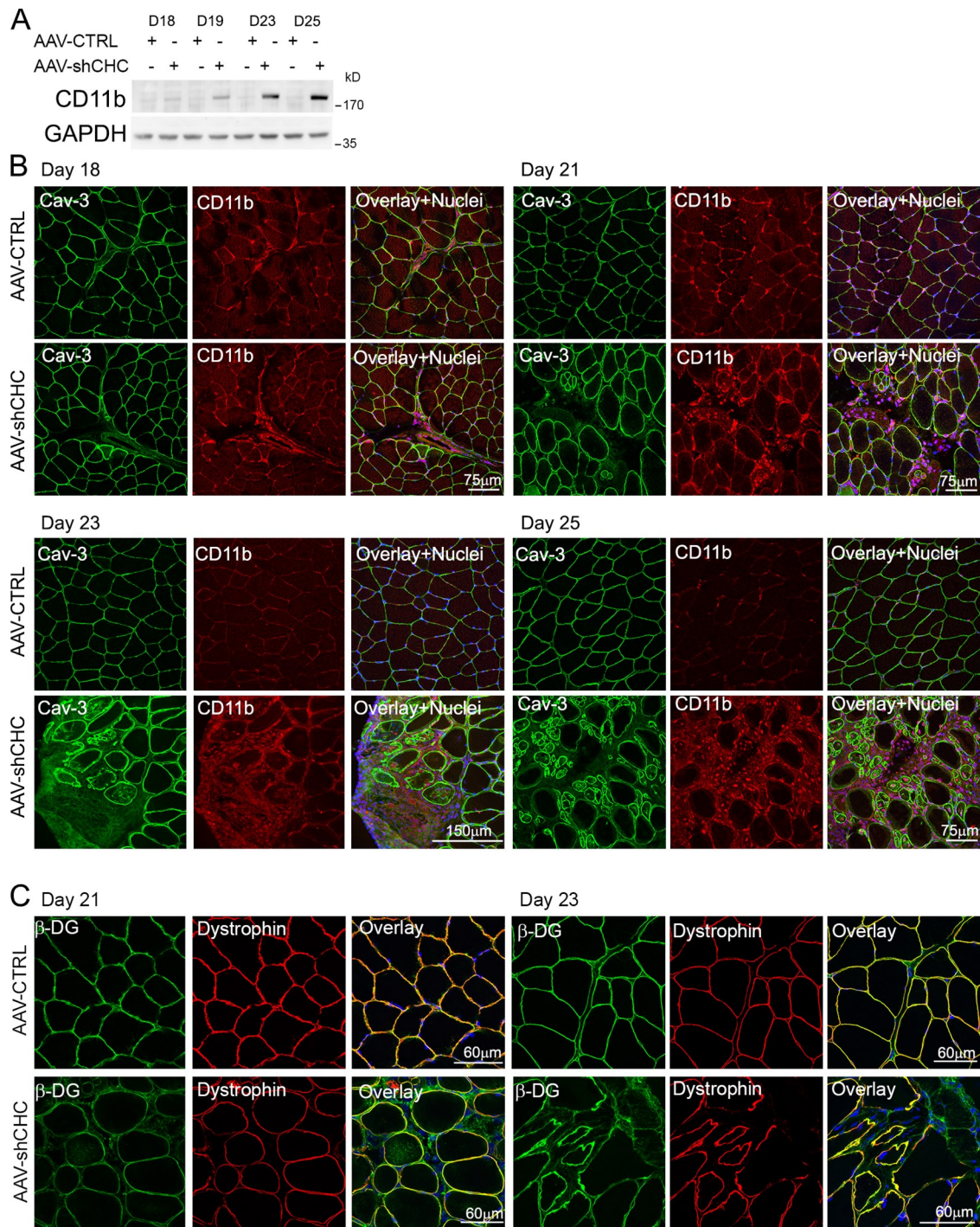


Figure S5. **CHC depletion induces a strong inflammatory response and has no effect on  $\beta$ -dystroglycan and dystrophin distribution.** (A) Western blot analysis of CD11b protein levels at 18, 19, 23, or 25 d after AAV-CTRL or AAV-shCHC injection. The D23 and D25 time points of this Western blot were previously shown in Fig. 8 C. GAPDH serves as a loading control. (B) Confocal microscopy on transverse sections of skeletal muscle processed for double-immunofluorescent labeling using antibodies against CD11b (red) and caveolin-3 (green, used as a marker to delineate muscle fibers) at day 18, 21, 23, and 25 PI. The overlay shows these images overlapped in color and in addition contains the DNA staining (DAPI, blue). (C) Confocal microscopy on transverse sections of skeletal muscle processed for double-immunofluorescent labeling using antibodies against  $\beta$ -dystroglycan (green) and dystrophin (red) at day 21 and 23 PI.